Article

Integration of Prognostics and Control of an Oil/CO$_2$ Subsea Separation System

Lucas Ferreira Bernardino [1], **André Felipe Ferreira de Souza [1]**, **Argimiro Resende Secchi [1,*]**, **Maurício Bezerra de Souza Jr. [1,2]** and **Anne Barros [3]**

[1] Programa de Engenharia Química, UFRJ, Rio de Janeiro 21941-450, Brazil; lbernardino@peq.coppe.ufrj.br (L.F.B.); andref@peq.coppe.ufrj.br (A.F.F.d.S.); mbsj@eq.ufrj.br (M.B.d.S.J.)

[2] Escola de Química, UFRJ, Rio de Janeiro 21941-909, Brazil

[3] Department of Mechanical and Industrial Engineering, NTNU, 7491 Trondheim, Norway; anne.barros@ntnu.no

* Correspondence: arge@peq.coppe.ufrj.br; Tel.: +55-21-25628307

Abstract: The exploitation of reserves with a high CO$_2$ content is challenging because of the need for its separation and the environmental impact associated with its generation. In this context, a suitable use for the generated CO$_2$ is its reinjection into the reservoir, and subsea CO$_2$ separation improves the efficiency of this process. The main objective of this work is to investigate the health-aware control of a subsea CO$_2$ separation system. Previously identified linear models were used in a predictive controller with Kalman filter-based state estimation and online model update, and simulations were performed to evaluate the controller tuning. Regarding prognostics, a stochastic model of pump degradation, sensitive to its operating conditions, was proposed, and a particle filter was implemented to perform online degradation state estimation and remaining useful lifetime prediction. Finally, a health-aware controller was designed, which could extend the life of the process by four months when compared to operation with a conventional model predictive controller. Some difficulties in combining reference tracking and lifetime extension objectives were also investigated. The obtained results indicate that dealing with the control problem through the multiobjective optimization theory or addressing the lifetime extension in an optimization layer may improve its performance.

Keywords: predictive control; equipment reliability; remaining useful lifetime; statistic inference; subsea processing

1. Introduction

In the context of process systems engineering, plant automation extends control possibilities and allows for operations in places virtually inaccessible to humans. The subsea environment is a classic example of an inaccessible place in which process operation is performed, mostly related to oil and gas exploitation in deep and ultradeep waters. Another issue that arises with low accessibility is maintenance planning, which needs to be done in order to prevent process interventions and production downtime, but also needs to take into account the difficulty of performing such maintenance. For this, reliability analysis aims to quantify rate or probability of casualties, in order to aid in the decision-making process [1].

In the early industrial periods, maintenance was done only at process breakdown ("run-to-failure maintenance"). This behavior often leads to major financial losses, so this kind of maintenance has mostly given way to preventive maintenance, in which parts are repaired or replaced based on historical data. As competition in the industries became tighter, the time between repairs became a critical variable. If this time interval is too high, the chances of a process breakdown rise. If it is too low,

maintenance costs become unfeasible. Traditional reliability-based preventive maintenance focused on the equipment population data, not on specific units with specific operational routines [2]. In order to assess these issues, the condition-based maintenance (CBM), a new paradigm of process maintenance, arises: interventions are made only when necessary, and equipment conditions are monitored in order to define if maintenance is necessary or not [3].

In the established CBM philosophy, the analyst essentially aims to estimate the remaining useful lifetime (RUL) of equipment. To attain this, health indicators are constructed from available system data, and with predefined degradation stages and failure thresholds, the indicators are projected into a time horizon [4]. The RUL of a given piece of equipment is defined as the time instant in which the respective health indicator exceeds its failure threshold, and prognostics is defined as the prediction of this RUL from process data [5].

This definition is well behaved in deterministic frameworks; however, as the reliability analysis deals with stochastic events, reliability metrics such as RUL are best described by probability distribution functions (p.d.f.) [6]. Therefore, the analyst should be aware that health monitoring information is inherently linked to a confidence level, and inappropriate confidence level selection can lead to false-positive or false-negative results.

Lei et al. [4] emphasize that Bayesian filtering algorithms are useful tools for characterizing uncertainty of the estimated health status and predicted RUL, being applicable to many prognostics strategies. However, Bayesian filtering needs to be used in tandem with a dynamic model, to enable propagation of the current estimated state through time to the critical state of the system. Particle filtering applied to prognostics is a recent trend in the literature. In 2006, Kothamasu et al. [7] performed a prognostics and health monitoring review, and particle filter use was not reported. Ten years later, Jouin et al. [8] reported the application of particle filters in prognostics and health monitoring, highlighting their generality in the face of nonlinear dynamic models and non-Gaussian probability distributions.

Reserves with high CO_2 content represent over 10% of the world's proven reserves. The exploitation of these fields generates major CO_2 quantities, which have low economic value and are an environmental burden, and must be separated in order to recover the main products with the required specifications. In this context, a suitable destination for CO_2 is its reinjection into the reservoir, in order to increase the oil recovery factor and thus oil production over the years [9].

In this sense, the early separation of CO_2 from the oil stream is beneficial, because downstream equipment can be sized for lesser flow rates, and produced CO_2 can be readily reinjected into the reservoir. This strategy, known as HISEP^{TM}, was first addressed by Petrobras. Passarelli [10] and Passarelli et al. [11] proposed a subsea CO_2 separation process that takes advantage of mixture thermodynamic properties in well conditions to ensure phase separation and good hydrocarbon recovery to the topside. Souza [12] and Souza et al. [13] analyzed the technical feasibility of this process and developed a dynamic model inspired by it.

CO_2 reinjection requires the use of a submersible pump able to promote a considerable pressure rise. Therefore, as this piece of equipment operates under the harshest conditions, it is reasonable to assume that process failure is most likely to happen in the pump, and thus, degradation modeling efforts in this work shall be directed towards it.

The general objective of this work is to investigate the main aspects of the development of a health-aware control (HAC) tool, which performs control, prognostics, and optimization, applied to a subsea CO_2 separation system model. More specifically, this work aims to assess the process control and prognostics, and how they can be combined. This paradigm is new in the literature, and although some effort has been put into dealing with these issues (see [14–19]), there is no consensus on how to optimally solve HAC problems.

The present work intends to present contributions in terms of control, prognostics, and application. The developed HAC approach is innovative in terms of its formulation, expanding the traditional model predictive control algorithm to include an explicit health-aware compromise. Additionally,

the introduced prognostic is based on a new, original stochastic dynamic degradation model, and a particle filter, which performs online state estimation based on the model. Finally, the application focuses on a new HISEP^{TM} process of high CO_2 percentage separation. There are no published works in the open literature of HAC of this process, as it is a technology that is being developed right now.

2. Methodology

In this section, the studied process and the methods related to its control and prognostics are detailed.

2.1. Process Description

The process flow diagram (PFD) for the process considered in this work is displayed in Figure 1. This PFD is based on a process conception developed by Passarelli [10] and further analyzed by Souza [12] and Souza et al. [13].
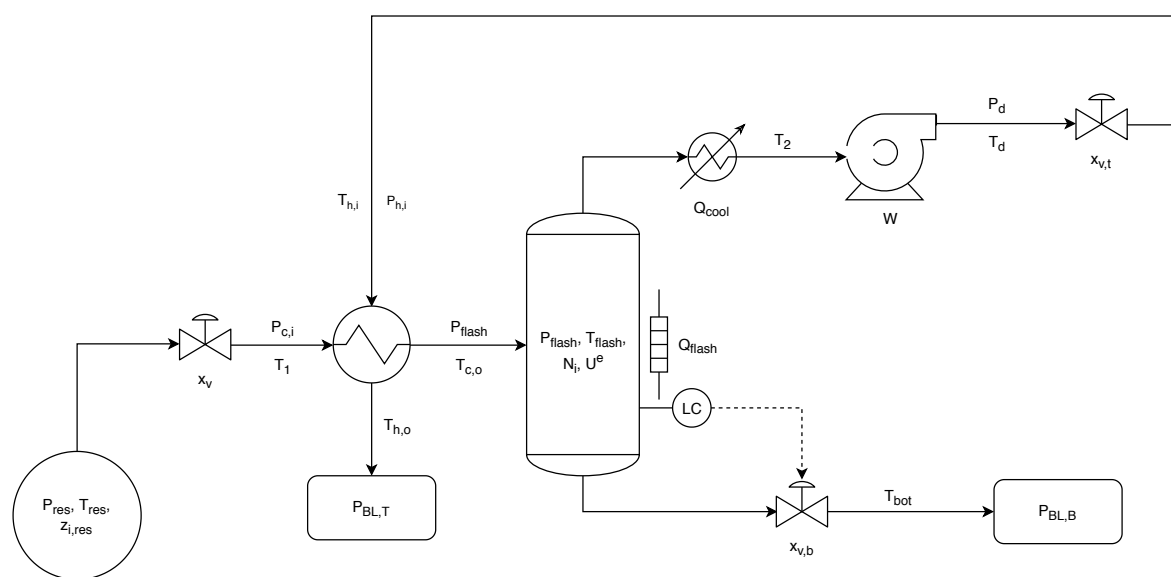

Figure 1. Process diagram, emphasizing correspondent variables [20].

In this process, the crude oil in reservoir conditions is submitted to heat exchange with a hot stream from the process, which provides part of the heat necessary for separation. This stream is then sent to a separator drum, in which the remaining heat necessary for separation is provided. The CO_2 rich stream, withdrawn at the top outlet, is cooled, elevating its density so that it becomes adequate for pump operation. The pump elevates the fluid pressure, allowing its reinjection, but it also significantly raises the fluid temperature. This temperature elevation enables heat integration between this stream and the crude oil extracted from the reservoir. After heat integration, the CO_2 rich stream is sent to the reinjection section. The separation drum bottom stream is then sent to topside processing. In addition, to stabilize the process, a proportional integral (PI) controller is implemented to control the flash drum liquid content by manipulating the bottom valve opening.

The dynamic model for the system studied in this work and the process variables are detailed in Appendix A. Simulations were carried out in Python 3.7 [22]. The *CO$_2$Therm* package developed by Souza [12] was interfaced to Python using the *Boost:Python* library [21]. Differential-algebraic equation system integration was performed using the Implicit Differential-Algebraic (IDA) algorithm from the Assimulo package [23].

2.2. Setpoint Tracking Control System

A discrete linear state-space dynamic model, with a sampling time of 10 s, was identified. The interested reader may find all the details of the linear identification in [20]. The identified

model was used as the internal model for the model predictive control (MPC) framework, in which the controlled variables were selected as $y = [F_{in}, P_{flash}, T_{flash}, T_2]$, and the manipulated variables were selected as $u = [x_{v,t}, x_v, Q_{flash}, Q_{cool}, W]$. This choice of controlled and manipulated variables was made according to a previous work [13], in which unconstrained MPC was compared with feedback control.

The implemented MPC framework comprises a discrete Kalman filter (KF), which was used to perform state estimation and model correction, and an optimizer used to calculate the optimal control actions sequence.

For the KF implementation, the temporal and measurement update equations were implemented as in Equations (1) and (2), respectively [24].

$$
\begin{cases}
P_k^- = F P_{k-1}^+ F^T + Q & \text{(1a)} \\
\hat{x}_k^- = F \hat{x}_{k-1}^+ + G u_{k-1} + w_{k-1} & \text{(1b)}
\end{cases}
$$

$$
\begin{cases}
K_k = P_k^- C^T (C P_k^- C^T + R)^{-1} & \text{(2a)} \\
P_k^+ = (I - K_k C) P_k^- & \text{(2b)} \\
\varphi_k = K_k (y_k - C \hat{x}_k^- - D u_k) & \text{(2c)} \\
\hat{x}_k^+ = \hat{x}_k^- + \varphi_k & \text{(2d)} \\
w_k = w_{k-1} + \varphi_k & \text{(2e)}
\end{cases}
$$

The dynamic optimization problem for the control actions calculations was formulated as in Equation (3). This optimization problem was solved using the *scipy.optimize.minimize* routine, using the sequential least squares programming (SLSQP) method (tolerance $ftol = 10^{-6}$) [25]. Tuning parameters for the control system were selected based on the literature for the MPC [26] and simulation tests. The used parameters are presented in Table 1.

$$
\min_{\Delta u_{k+j}} J = \sum_{i=1}^{N_y} \sum_{j=1}^{N_p} q_i^2 (\hat{y}_{i,k+j} - y_{i,k+j}^{sp})^2 + \sum_{i=1}^{N_u} \sum_{j=0}^{N_c-1} s_i^2 (\Delta u_{i,k+j})^2
$$

subject to: $\quad u_{k+j}^{min} \le u_{k+j} \le u_{k+j}^{max}, \quad j = 0, \cdots, N_c - 1$ (3)

$\qquad\qquad\quad -\Delta u_{k+j}^{max} \le \Delta u_{k+j} \le \Delta u_{k+j}^{max}, \quad j = 0, \cdots, N_c - 1$

$\qquad\qquad\quad x_{k+j} = F x_{k+j-1} + G u_{k+j-1} + w_k, \quad j = 1, \cdots, N_p$

$\qquad\qquad\quad \hat{y}_{k+j} = C x_{k+j} + D u_{k+j}, \quad j = 1, \cdots, N_p$

Table 1. Kalman filter (KF) and model predictive control (MPC) tuning parameters (units consistent with values of Tables A2 and A3).

| Q | R | q_i | | s_i | N_p | N_c |
		F_{in}	$P_{flash}, T_{flash}, T_2$			
I	diag(0.001 y^{ss})	10	1	10	75	10

With this setup, closed-loop simulations were performed to evaluate the performance of the controller with the proposed tuning. All dynamic simulations had the nominal steady state, described in Appendix A, as the initial condition, and at t = 0, a change in the flash drum pressure setpoint of +0.5 MPa was implemented.

2.3. Prognostics Module

The implemented prognostics module comprises a stochastic dynamic model, which represents the pump degradation process as a function of its operating point, and a sequential importance resampling (SIR) particle filter, which performs online state estimation based on the degradation model [27].

The degradation state evolution (λ) was modeled inspired by Paris' law for crack propagation [28] and is given by Equation (4), in which the p.d.f. corresponds to a $Gamma(k, \theta)$ distribution as defined by Equation (5), and W_k represents the pump operating power at time k.

$$\lambda_{k+1} = \lambda_k + \Delta f_k \lambda_k^n, \qquad \Delta f_k \sim Gamma(\theta_1 W_k \Delta t, \theta_2) \tag{4}$$

$$Gamma(x|k, \theta) = \frac{x^{k-1}}{\Gamma(k)\theta^k} e^{-\frac{x}{\theta}} \tag{5}$$

The considered observation for the degradation system is the degradation state, corrupted by white noise, according to Equation (6).

$$\eta_k = \lambda_k + \epsilon_k, \qquad \epsilon_k \sim \mathcal{N}(0, \sigma^2) \tag{6}$$

Table 2 presents the parameters for the degradation model. For this set of parameters, the operational degradation limit was fixed as $\lambda^{lim} = 1.0$.

Table 2. Degradation model parameters.

λ_0	Δt	$\theta_1 \ (MJ^{-1})$	θ_2	n	σ
0.001	0.05 year	5×10^{-7}	0.01	0.7	0.0001

The particle filter was implemented with the same model and parameter set as the considered degradation process, except from the standard deviation, which was considered to be $\sigma = 0.001$. The algorithm was based on Speekenbrink [27], and is further described in Appendix B. The number of particles was $N_{part} = 100$, the resampling rate was $c = 0.5$, and particles at time $k = 0$ were sampled from $\mathcal{N}(0.001, 10^{-10})$. All statistical operations were performed using the *scipy.stats* algorithms.

Simulations of the degradation process were performed considering a planned horizon for the manipulation of the pump power W. Using the filter results, a prediction of RUL was made at each measurement. To evaluate prediction performance, this was compared to the actual end-of-life time in the simulation.

2.4. Health-Aware Control System

By combining the setpoint tracking control system and the prognostics module, an HAC structure was implemented. It consists of an MPC, with the objective function written as in Equation (7), with w_{HAC} being the weighting factor between RUL extension and control objectives, and $\overline{RUL}$ being the average of RUL between the propagated particles. Tuning parameters were kept as in Table 1.

$$J_{HAC} = -w_{HAC}\overline{RUL} + \sum_{i=1}^{N_y}\sum_{j=1}^{N_p} q_i^2 (\hat{y}_{i,k+j} - y_{i,k+j}^{sp})^2 + \sum_{i=1}^{N_u}\sum_{j=0}^{N_c-1} s_i^2 (\Delta u_{i,k+j})^2 \tag{7}$$

The model proposed in Equation (4), however, cannot be directly used in a deterministic optimization problem, due to its randomness. Furthermore, as the degradation model is represented in discrete time, $\overline{RUL}$ has no direct correlation in continuous space. To address these issues, the strategy used to calculate $\overline{RUL}$ during the optimization procedure is as given in Algorithm 1.

Algorithm 1: $\overline{RUL}$ calculation

Data: $\lambda_0^{(i)}$ $(i = 1, \cdots, N_{part})$, λ^{lim}, $\mu_k^{(i)}$ $(i = 1, \cdots, N_{part}, \ k = 0, \cdots)$, W_{end}

Result: $\overline{RUL}$

1 **for** $i \leftarrow 1$ **to** N_{part} **do**

2 $\quad$ $k \leftarrow 0$;

3 $\quad$ **while** $\lambda_k^{(i)} < \lambda^{lim}$ **do**

4 $\quad\quad$ $\Delta f_k^{(i)} \leftarrow Q(\mu_k^{(i)}, W_{end})$;

5 $\quad\quad$ $\lambda_{k+1}^{(i)} \leftarrow \lambda_k^{(i)} + \Delta f_k^{(i)} (\lambda_k^{(i)})^n$;

6 $\quad\quad$ $k \leftarrow k + 1$;

7 $\quad$ **end**

8 $\quad$ $RUL^{(i)} \leftarrow k - \dfrac{\lambda_k^{(i)} - \lambda^{lim}}{\lambda_k^{(i)} - \lambda_{k-1}^{(i)}}$;

9 **end**

10 $\overline{RUL} \leftarrow \sum_{i=1}^{N_{part}} RUL^{(i)} / N_{part}$;

In Algorithm 1, $\mu_k^{(i)}$ represents the quantile associated with the *k*-th evolution of the *i*-th particle, W_{end} represents pump power at the end of the control horizon, and $Q(\cdot)$ represents the inverse cumulative distribution function associated with the distribution in Equation (4), depending on the pump power which varies along the optimization. The set of $\mu_k^{(i)}$ is sampled from a standard uniform distribution, and kept constant in the optimization course. As a result of the difference between timescales, W_{end} was considered as the dominant effect in the degradation pattern, and the variation during the control horizon can be neglected.

For simplicity, the MPC internal model was considered to be representative of the process, being used as the process model. The used MPC tuning was the same as described in Table 1, except for the control horizon, which was $N_c = 2$. For higher control horizons, the optimization problem is ill-posed.

Closed-loop simulations were performed to evaluate the influence of the number of particles (N_{part}) and the value of w_{HAC}, in Equation (7), over the controller performance.

3. Results and Discussion

3.1. Setpoint Tracking Control System

In order to attain the main objective, which is to develop an HAC tool, first it is necessary to evaluate the system control separately. Guaranteeing that the controller is well tuned is fundamental before adding complexity to the control framework. Furthermore, these results serve as a benchmark for the proposed HAC framework.

Figure 2 presents the closed-loop simulation results for a setpoint change of the flash drum pressure. System settling occurred at around 600 s, which justifies the chosen prediction horizon of 750 s. The implemented controller produced no offset, even though there is a mismatch between the controller internal model and the plant. This result is due to the KF-based model update translated in the variable w. For comparison, the same simulation without the model update, i.e., $w_k = 0 \ \forall k$, is also displayed, in which an offset can be observed. This highlights the importance of feedback, not only in state estimate, but in the process internal model in order to attain a good performance in the control strategies. The adopted model update, although simple, was enough to represent the process nonlinearities that come with the steady state change.
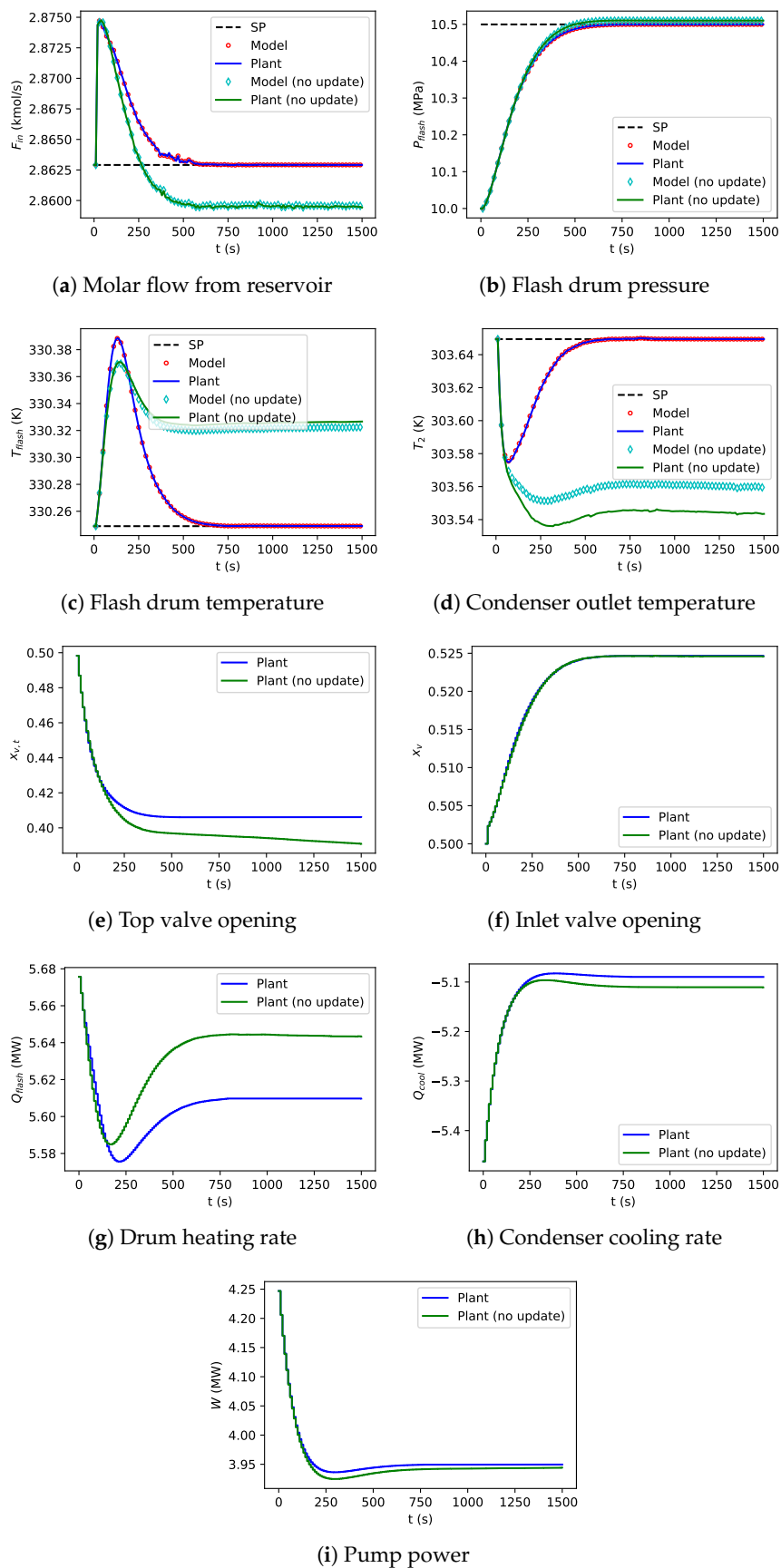
(**a**) Molar flow from reservoir

(**b**) Flash drum pressure

(**c**) Flash drum temperature

(**d**) Condenser outlet temperature

(**e**) Top valve opening

(**f**) Inlet valve opening

(**g**) Drum heating rate

(**h**) Condenser cooling rate

(**i**) Pump power

Figure 2. Closed-loop simulation of the flash pressure setpoint change: effect of the KF model update.

3.2. Prognostics Module

Using a representative model of the degradation process, online state estimation was performed using a particle filter. Despite the fact that a simple tool such as the Kalman filter was used for the process control problem, the prognostics problem requires a more sophisticated tool. This is due to the absence of a representative linear model of the degradation process, and the importance of keeping the statistical information of the model.

In the first set of simulations, a constant pump power corresponding to its nominal value ($W(t) = 4.246$ MW) was considered. Figures 3 and 4 present the results of the SIR filter implementation for the a priori and a posteriori distributions, respectively. It can be seen that the distributions remain well conditioned throughout the simulation due to the resampling step. Furthermore, as expected, the measurement update effectively narrows the sample distribution a posteriori, as the a priori information is combined with the measurement likelihood function, leading to smaller confidence regions for the degradation state.
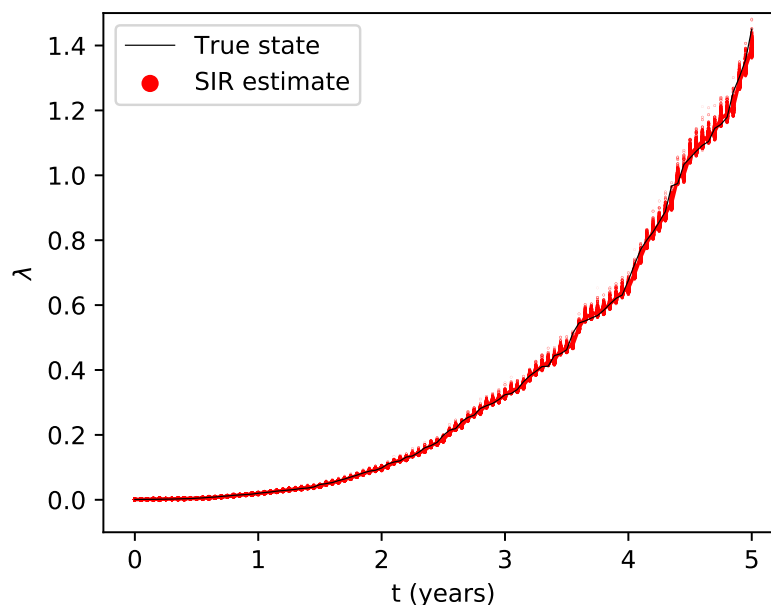

Figure 3. Degradation state online estimation—a priori distribution (dot size represents particle weight).

All parameters from the stochastic model were implemented in the particle filter as their actual values, meaning that no influence of modeling error was considered in this implementation. Only the likelihood function standard deviation was changed to $\sigma = 0.001$, solely due to numerical issues related to the very narrow actual likelihood function. This led to a more permissive filter, which means that *a posteriori* distributions are wider than necessary to describe the state.

Using the particle filter framework, RUL predictions can be performed. However, as RUL prediction generally involves a high number of state transitions, leading to high-dimensional statistical problems, it is known that a distribution reconstruction using importance sampling is nearly infeasible. The chosen strategy, then, was to retrieve information about the distributions by standard Monte Carlo sampling. As a discrete-time state transition model was used, predicted RUL belongs to a discrete set. Thus, the very number of occurrences of each realization was considered as representative of the probability.
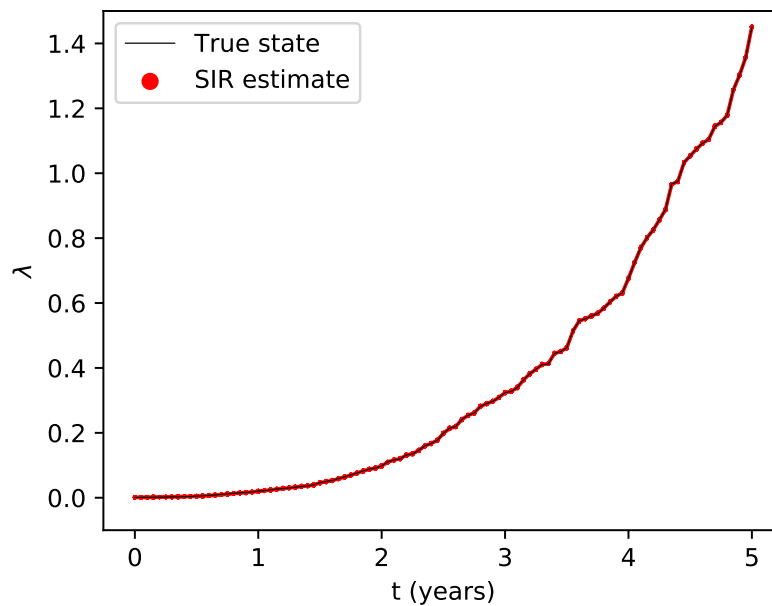
Figure 4. Degradation state online estimation—a posteriori distribution (dot size represents particle weight).

Results of RUL prediction for the SIR filter are presented in Figure 5, in which predicted RUL is displayed in terms of the number of discrete model evolution steps. It can be seen that SIR filter RUL distribution narrows around the true RUL as time passes. This is due to the resampling step, which redistributes particles in the most likely state values.
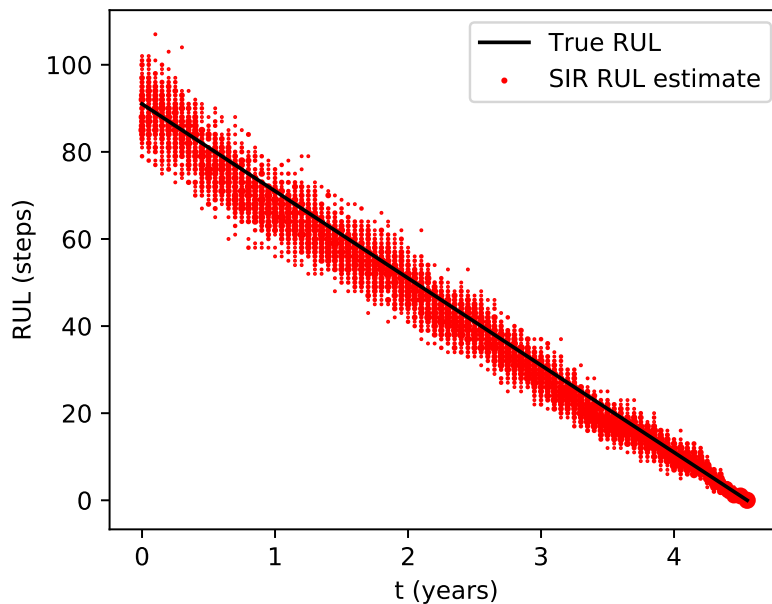

Figure 5. Remaining useful lifetime (RUL) prediction—sequential importance resampling (SIR) filter (dot size represents probability).

A simulation with time-varying pump power was also performed ($W(t) = 10.615 \times (5 - t)/5$ MW, t in years). Figures 6 and 7 show results for the sequential importance resampling (SIR) filter in the cases of a priori and a posteriori estimates, respectively. It can be seen that, for the a priori estimates, the distribution starts to degenerate when lower pump power is applied. This is due to the lack

of degradation in this region. Nevertheless, a posteriori weights are normalized and this effect is counteracted.
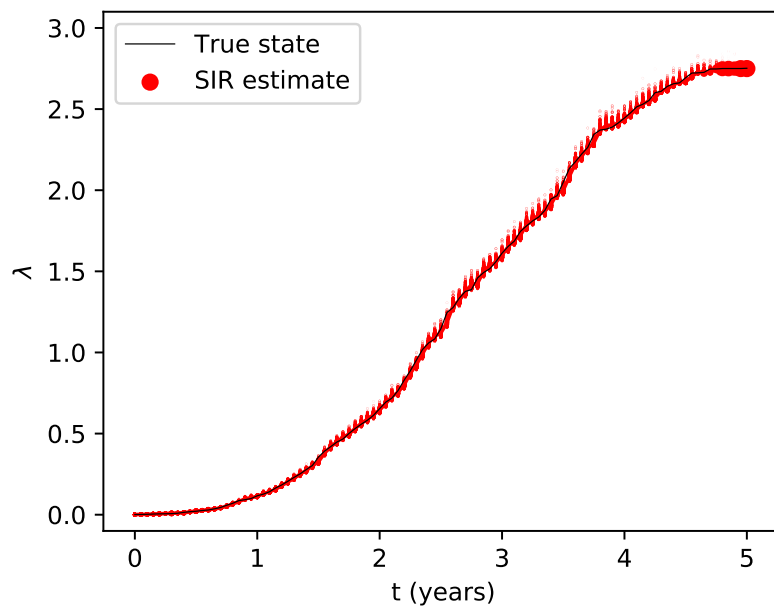

Figure 6. Degradation state online estimation with time-varying pump power—a priori distribution (dot size represents particle weight).
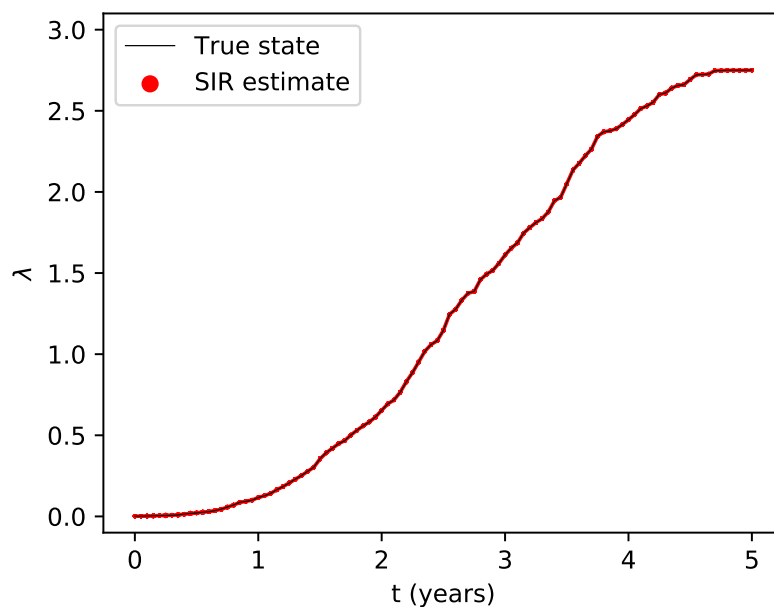

Figure 7. Degradation state online estimation with time-varying pump power—a posteriori distribution (dot size represents particle weight).

Regarding the RUL prediction for this case, results for the SIR filter are given in Figure 8. Even though RUL prediction in early states is biased, as new measurements are incorporated, the predictions progressively become more accurate. This result encourages the use of particle filters as auxiliary tools in RUL prediction, even in the presence of modeling errors.
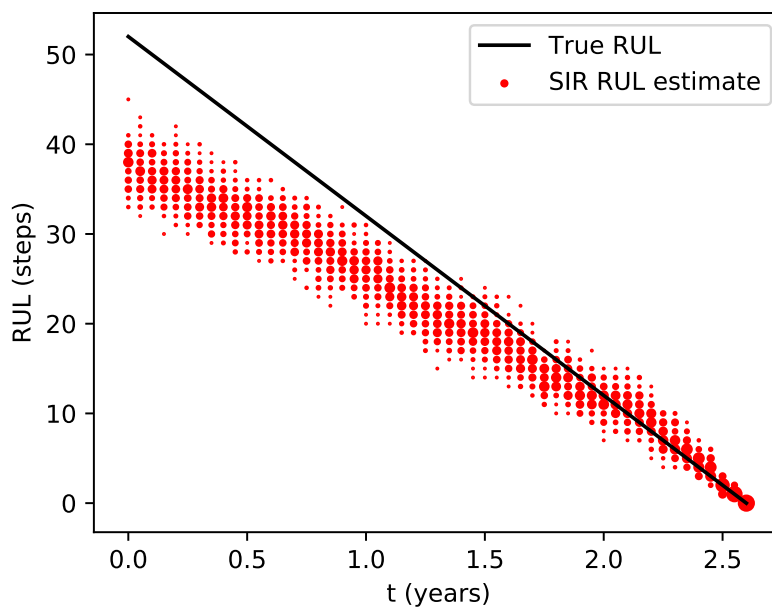
Figure 8. RUL prediction with time-varying pump power—SIR filter (dot size represents probability).

3.3. Health-Aware Control System

The HAC objective function described in Equation (7) aims to combine the health extension and control objectives in the same optimization problem. As the control problem has four independent controlled variables and five independent manipulated variables, there are enough degrees of freedom to find an operating point which satisfies the control objectives with the maximum equipment RUL. It is evident from the models that one should aim for the maximum top valve opening ($x_{v,t}$) to minimize pump effort and thus extend its lifetime.

The influence of w_{HAC} over the HAC strategy is explored in the simulations presented in Figures 9 and 10, with lower and higher values of w_{HAC}, respectively. As a result of the randomness of sampling $\mu_k^{(i)}$ at each control step, the RUL estimate ($\overline{RUL}$) fluctuates at each control action calculation, which changes the optimization problem at each time step and thus makes the attainment of a steady state impossible. As expected, the variable $x_{v,t}$ is brought to its allowed maximum, and W is minimized to some extent in all cases. In the case with lower w_{HAC}, even though the control objectives are not ignored, an offset is produced. As the operation reaches a point where health and control objectives compete against each other, the obtained solution is a compromise between these objectives. In the case with higher w_{HAC}, the optimization problem prioritized the RUL extension objective over the control objective to the point where the system diverges from the reference trajectory.

When stochastic problems are solved by sampling strategies such as particle filters, the number of samples is a key tuning parameter to attain an acceptable performance. As such, strategies to reduce the noise associated with sampling were investigated, and the results are summarized in Figure 11. By increasing the number of particles from 3 to 20, some reduction in the oscillation amplitude of $\overline{RUL}$ is observed. This means that the number of particles needs to be raised some orders of magnitude to attain a representative mean value that stays constant with the resetting of quantile samples.

As the elevation of the number of particles proved to be not very effective in stopping oscillatory behavior, a different strategy was adopted. Instead of resetting the values of $\mu_k^{(i)}$ at each control step, these values were kept constant throughout the closed-loop simulation. For this approach, the attainment of a noise-free steady-state value for the manipulated variables is evidenced, at the expense of a biased $\overline{RUL}$.

(**a**) Molar flow from reservoir

(**b**) Flash drum pressure

(**c**) Flash drum temperature

(**d**) Condenser outlet temperature

(**e**) $\overline{RUL}$

(**f**) Top valve opening

(**g**) Inlet valve opening

(**h**) Drum heating rate

(**i**) Condenser cooling rate

(**j**) Pump power
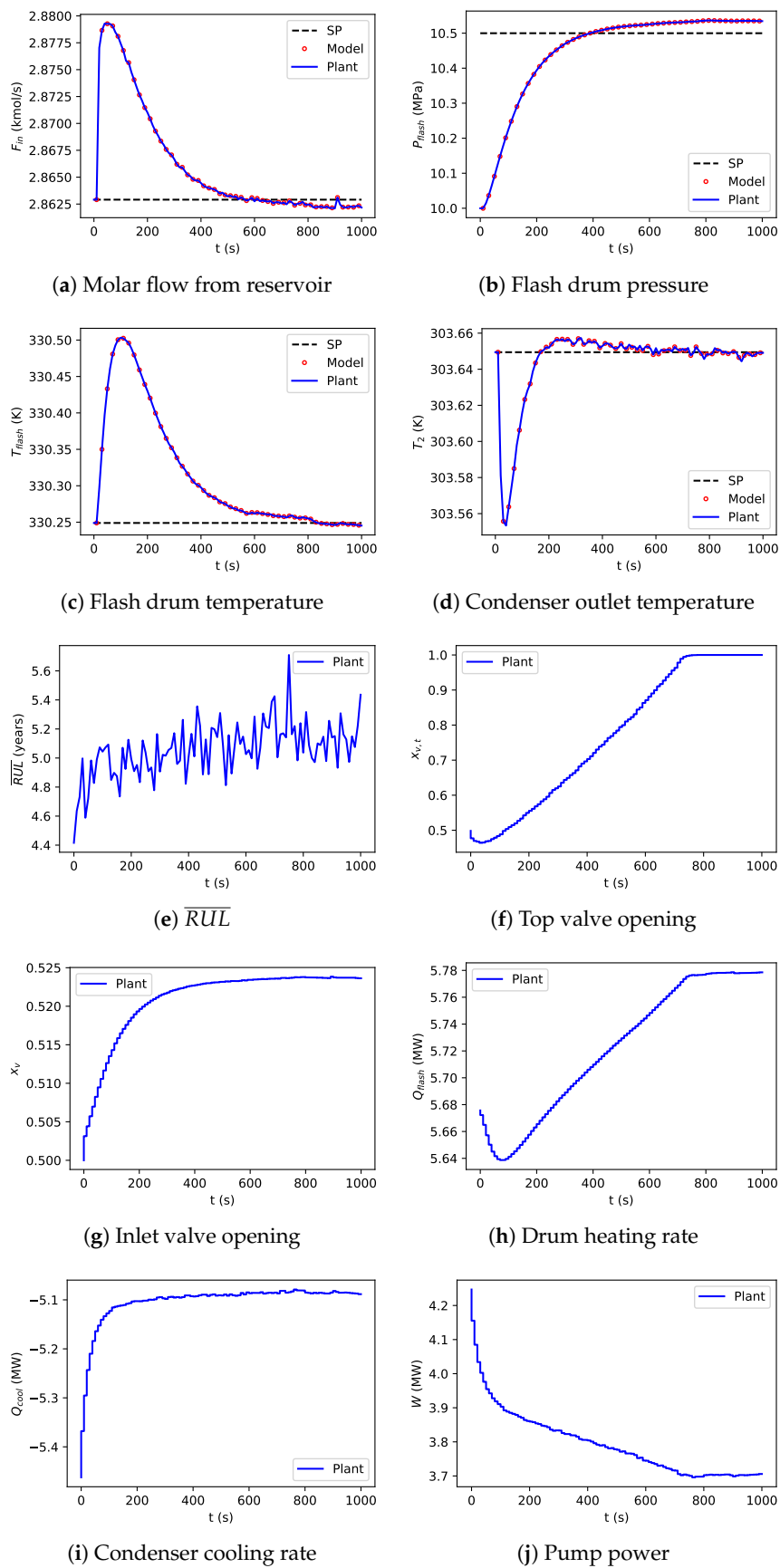
Figure 9. Health-aware control (HAC) simulation—$w_{HAC} = 5$, $N_{part} = 3$.

(**a**) Molar flow from reservoir

(**b**) Flash drum pressure

(**c**) Flash drum temperature

(**d**) Condenser outlet temperature

(**e**) $\overline{RUL}$

(**f**) Top valve opening

(**g**) Inlet valve opening

(**h**) Drum heating rate

(**i**) Condenser cooling rate
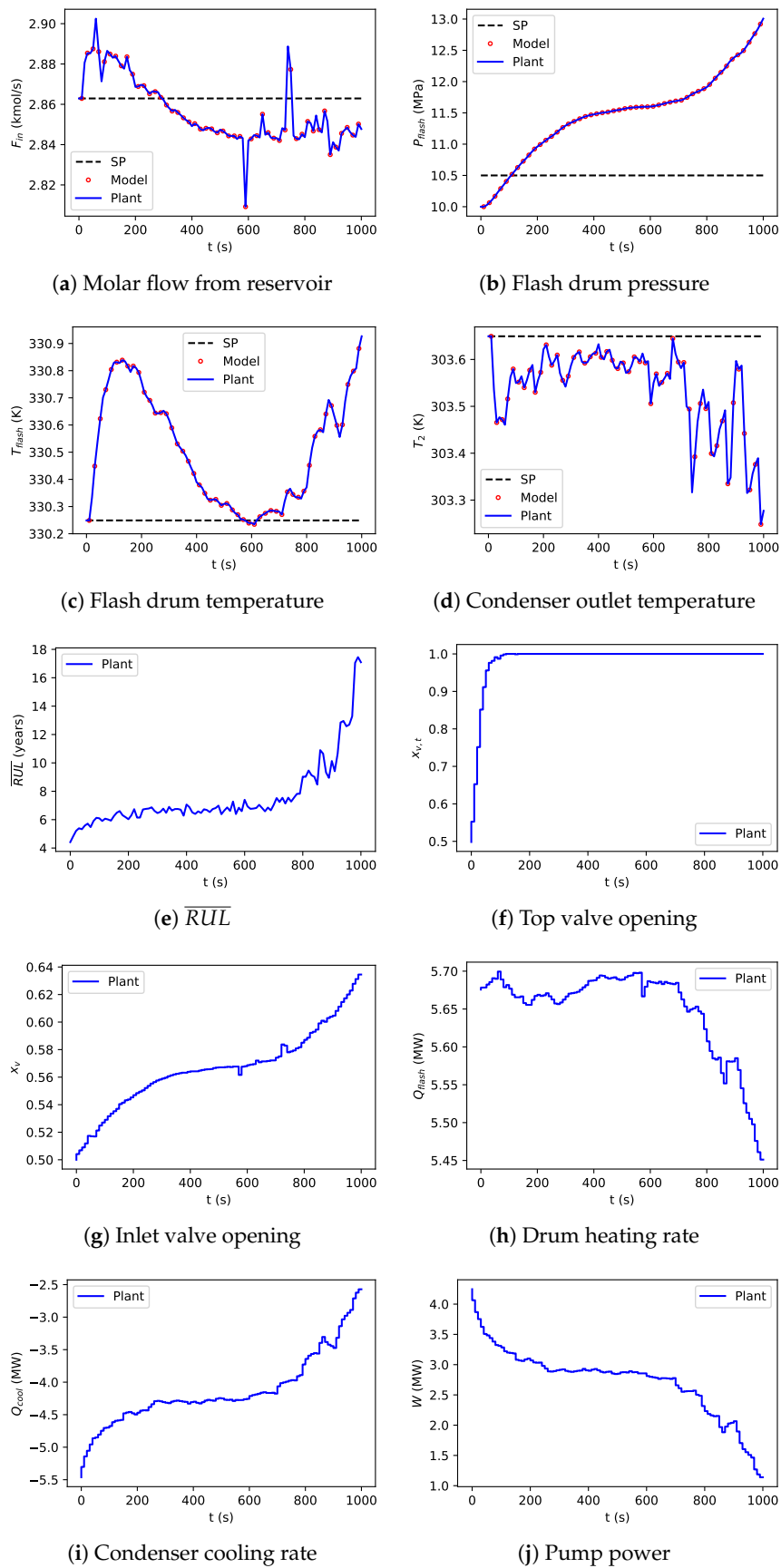
(**j**) Pump power

Figure 10. HAC simulation—$w_{HAC} = 100$, $N_{part} = 3$.

For comparison purposes, the results presented in Figure 2, which correspond to an HAC controller with $w_{HAC} = 0$, are complemented with the corresponding $\overline{RUL}$ presented in Figure 11. The difference between the steady $\overline{RUL}$ of HAC and MPC highlights the RUL extension capability of the HAC strategy.
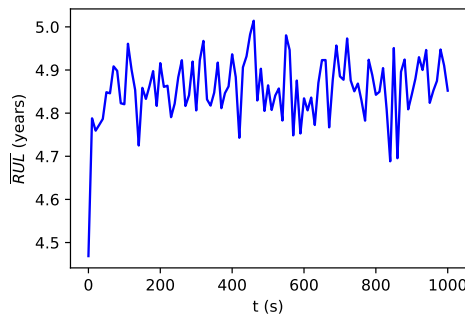

Figure 11. $\overline{RUL}$ corresponding to the MPC simulation (Figure 2).

In all of the presented HAC simulations, it was not possible to eliminate the offset when the health extension objective conflicts with the reference tracking objective. This suggests that a different approach is necessary to attain both objectives.

4. Conclusions

In this work, motivated by the recently developed process of subsea CO_2 separation, process modeling, control strategies, and equipment prognostics were assessed.

The control strategies employed in this work were the PI controller, whose main role was to stabilize plant dynamic behavior, in parallel with an MPC controller, with a linear internal model identified from the PI-stabilized plant, and a KF, used to correct state estimates and model bias. This strategy was successful, highlighting the importance of filter-based model correction in cases of model–plant mismatch.

A pump wear model was proposed, which reunited most of the desired characteristics in an equipment wear model (monotonicity, time independence, dependence with important operational variables). Using the stochastic processes mathematical formulation, particle filters were successfully used to estimate states and predict the remaining useful lifetime. The development of this kind of model is challenging mainly because of the scarcity of quality data regarding all of the relevant variables. This development was however very encouraging because of the positive impact it can have on process reliability and optimization.

The main achievements of this work were then consolidated in the deployment of an HAC tool to solve the proposed case study. For the case with $w_{HAC} = 10$ (Figure 12), the tool was able to extend the lifetime of the process by roughly 4 months, compared to the same operation with a conventional MPC (Figure 11) when the process is still under healthy conditions. Even though consistent results were obtained, some limitations of the proposed method were noted, most of them concerning the contraposition of health and control objectives.

The unstable behavior seen with the high RUL extension priority is a known issue which has been explored in the development of economic MPCs. For this class of control problem, stability can be guaranteed under some assumptions and modifications of the optimization problem [29].

As any optimization problem with multiple conflicting objectives, the most accurate way to express it mathematically is as a multiobjective optimization problem. The objective function formulated in Eq. (7) can be seen as simply the multiobjective problem solved using the weighted sum approach. Therefore, the treatment of this generic problem using other tools, such as the goal attainment method [30], can result in more reasonable control policies.

(**a**) Molar flow from reservoir

(**b**) Flash drum pressure

(**c**) Flash drum temperature

(**d**) Condenser outlet temperature

(**e**) $\overline{RUL}$

(**f**) Top valve opening

(**g**) Inlet valve opening

(**h**) Drum heating rate

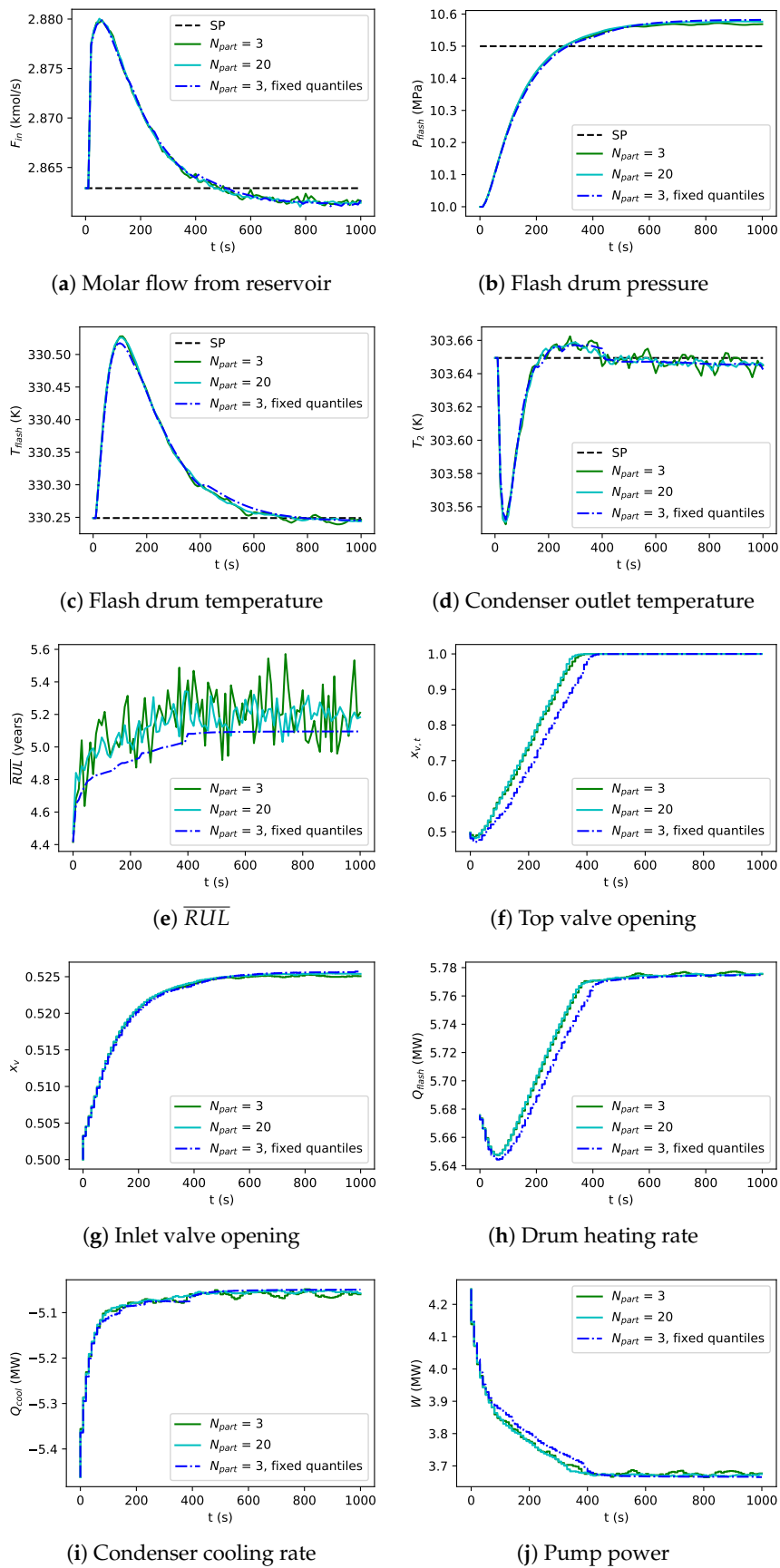(**i**) Condenser cooling rate

(**j**) Pump power

Figure 12. HAC simulations—evaluation of sampling noise ($w_{HAC} = 10$).

Although this problem was solved in an one-layer control framework, the complexity of the methods necessary to describe the degradation phenomenon suggests that this issue could in future investigative works be addressed in a higher control layer and a systematic comparison could be performed. With this, a higher number of particles could be used, resulting in not only a more reliable $\overline{RUL}$ estimation, but in an estimate of the RUL p.d.f. itself. This is expected to enable the analyst to work with the constraints related to the confidence level of the degradation process, resulting in a more robust decision-making.

Author Contributions: The main author L.F.B. conducted all the steps of the research that produced the results reported here, including: literature review, problem definition, computational implementation and simulations and generation of the results. He also led the writing step. A.F.F.d.S. participated in the development and refinement of the process model and simulation. A.R.S., M.B.d.S.J. and A.B. supervised the research, defining its scope, analyzing the results, and participating in the elaboration of the article for publication. All authors have read and agreed to the published version of the manuscript.

Conflicts of Interest: The authors declare no conflict of interest.

Appendix A. Process Model

In this section, the model of the subsea CO_2 separation system considered in this work is described. It is considered that the reservoir contains CO_2, water, methane, and heavy hydrocarbons modeled as pseudocomponents F_1, F_2, F_3, and F_4. The interested reader is encouraged to consult Bernardino [20] for a more thorough process description, and Souza [12] for the description of the thermodynamic package *CO$_2$Therm*.

Appendix A.1. Valves

A scheme which emphasizes variables of the valve model is presented on Figure A1.
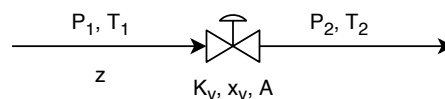

Figure A1. Valve scheme, emphasizing model variables.

For this model, it was assumed that the flow through a valve is an isenthalpic process, and that the molar flow has a linear correlation with the valve opening, as in

$$
\begin{cases}
H(T_1, P_1, z) = H(T_2, P_2, z) & \text{(A1a)} \\[2ex]
F = \dfrac{A}{MM(z)} K_v x_v \bar{\rho}_m \sqrt{\dfrac{\Delta P}{\bar{\rho}_m}} & \text{(A1b)} \\[2ex]
\bar{\rho}_m = \dfrac{-1}{\Delta P} \displaystyle\int_1^2 \rho_m dP, & \text{(A1c)}
\end{cases}
$$

in which A represents the valve cross-section area, x_v represents the valve opening, and K_v represents the valve constant.

Appendix A.2. Heat Exchanger

The heat exchanger used for process integration was discretized into theoretical stages, as depicted in Figure A2.
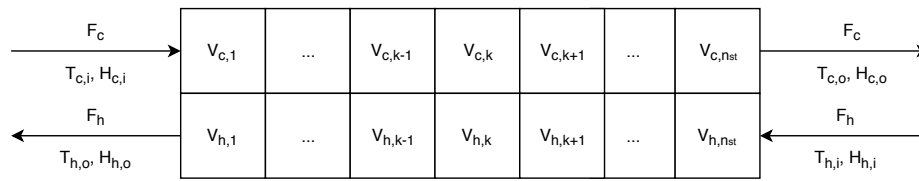
Figure A2. Heat exchanger discretization scheme, emphasizing model variables.

By performing energy balances at each theoretical stage, the following equations apply:

$$
\begin{cases}
\dfrac{dE_{c,k}}{dt} = F_c(H_{c,k-1} - H_{c,k}) + UA_k(T_{h,k} - T_{c,k}) & \text{(A2a)} \\[3mm]
\dfrac{dE_{h,k}}{dt} = F_h(H_{h,k+1} - H_{h,k}) - UA_k(T_{h,k} - T_{c,k}), \quad k = 1, \cdots, n_{st} & \text{(A2b)} \\[3mm]
E_{c,k} = V_{c,k}\rho_{c,k}H_{c,k} & \text{(A2c)} \\[3mm]
E_{h,k} = V_{h,k}\rho_{h,k}H_{h,k}, & \text{(A2d)}
\end{cases}
$$

with n_{st} being the number of theoretical stages.

Appendix A.3. Flash Drum

The flash drum modeled in this work is schematized in Figure A3.

Figure A3. Flash drum scheme, emphasizing model variables.

The equation system that models this equipment is written as

$$
\begin{cases}
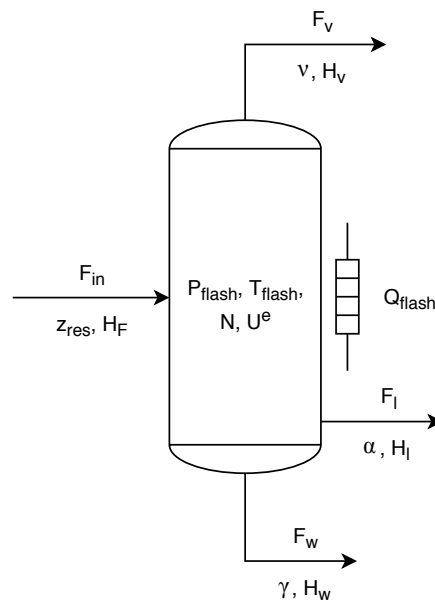\dfrac{dN_i}{dt} = F_{in}z_{i,res} - F_v v_i - F_l \alpha_i - F_w \gamma_i, \qquad i = 1, \cdots, n_c & \text{(A3a)} \\[2ex]
\dfrac{dU^e}{dt} = F_{in}H_F - F_v H_v - F_l H_l - F_w H_w + Q_{flash} & \text{(A3b)} \\[2ex]
\dfrac{U^e + P_{flash}V_{flash}}{N_{tot}} = \beta_v H_v + \beta_\alpha H_l + \beta_\gamma H_w & \text{(A3c)} \\[2ex]
\dfrac{V_{flash}}{N_{tot}} = \beta_v \bar{V}_v + \beta_\alpha \bar{V}_l + \beta_\gamma \bar{V}_w & \text{(A3d)} \\[2ex]
[\beta_v, \beta_\alpha, \beta_\gamma, \boldsymbol{v}, \boldsymbol{\alpha}, \boldsymbol{\gamma}] = \text{Flash3P}(T_{flash}, P_{flash}, \boldsymbol{z}) & \text{(A3e)} \\[2ex]
z_i = \dfrac{N_i}{N_{tot}} & \text{(A3f)} \\[2ex]
N_{tot} = \displaystyle\sum_{i=1}^{n_c} N_i. & \text{(A3g)}
\end{cases}
$$

The model for this equipment comprises the component material balances and the energy balance. The thermodynamic package *CO₂Therm* [12] supplies the algorithm Flash3P, that performs (P, T) specified flash calculations. However, as the drum internal energy and volume are specified, algebraic constraints are necessary to ensure consistency.

The drum level is obtained from the liquid volumetric fraction at drum conditions, given by

$$
h_{flash} = \frac{(\beta_\alpha \bar{V}_l + \beta_\gamma \bar{V}_w)N_{tot}}{V_{flash}}. \tag{A4}
$$

Appendix A.4. Pump

The scheme for the submersible pump employed in this virtual plant is shown in Figure A4.
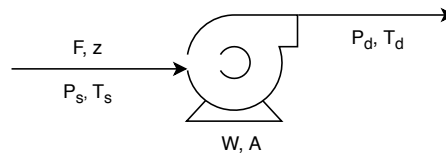
Figure A4. Pump scheme, emphasizing model variables.

The model for this equipment is composed of an energy balance (Bernoulli equation) and the assumption of isentropic flow, given respectively by

$$
\begin{cases}
W = F\left\{ MM(\boldsymbol{z})\left[\left(\dfrac{F\bar{V}_d}{A}\right)^2 - \left(\dfrac{F\bar{V}_s}{A}\right)^2\right] + \displaystyle\int_{P_s}^{P_d} \bar{V}dP \right\} & \text{(A5a)} \\[3ex]
H(T_d, P_d, \boldsymbol{z}) - H(T_s, P_s, \boldsymbol{z}) = \displaystyle\int_{P_s}^{P_d} \bar{V}dP. & \text{(A5b)}
\end{cases}
$$

Appendix A.5. PI Controller

The PI controller was implemented using the following formulation, in which the integral term is calculated through an auxiliary differential equation in time:

$$
\begin{cases}
x_{v,b} = k_c \left[(h_{sp} - h_{flash}) + \dfrac{\Psi}{\tau_I} \right] & \text{(A6a)} \\[4mm]
\dfrac{d\Psi}{dt} = h_{sp} - h_{flash}, \qquad \Psi(0) = \dfrac{x_{v,b}^{steady} \tau_I}{k_c}. & \text{(A6b)}
\end{cases}
$$

The controller was tuned using rules proposed by Skogestad [31] based on the identified transfer function of the pair $x_{v,b} \times h_{flash}$, with $\tau_c = 10\ s$.

Appendix A.6. Model Parameters

The parameters and variables presented in Tables A1 and A2 were used throughout all the simulations. Using these, the obtained nominal steady state is described by the variables in Table A3.

Table A1. Parameters used in the simulation.

Parameter	Value	Unit	Description
n_{st}	3	-	Number of heat exchanger theoretical stages
K_v	0.0982	-	Inlet valve constant
$K_{v,t}$	0.0564	-	Top valve constant
$K_{v,b}$	0.1589	-	Bottom valve constant
D	0.3048	m	Piping diameter
ΔP_h	0	MPa	Pressure drop of hot fluid (top stream)
ΔP_c	0	MPa	Pressure drop of cold fluid (inlet stream)
UA	0.153	MW/K	Overall heat transfer coefficient
V_{flash}	31.8086	m^3	Flash drum volume
V_c	1.806	m^3	Heat exchanger cold side volume
V_h	0.387	m^3	Heat exchanger hot side volume
k_c	−31.127	-	Proportional integral (PI) controller gain
τ_I	40	s	PI controller integral time constant

Table A2. Fixed variables used in the simulation.

Parameter		Value	Unit	Description
	H_2O	0.0100	-	
	CO_2	0.7500	-	
	CH_4	0.0480	-	
z_{res}	F_1	0.0543	-	Reservoir composition
	F_2	0.0443	-	
	F_3	0.0520	-	
	F_4	0.0413	-	
T_{res}		313.15	K	Reservoir temperature
P_{res}		15	MPa	Reservoir pressure
$P_{BL,B}$		9	MPa	Pressure at bottom side battery limit
$P_{BL,T}$		59	MPa	Pressure at top side battery limit

Table A3. Nominal conditions.

Parameter		Value	Unit	Description
$E_{c,k}$	1	−6.4567	10^7 J	
	2	−6.0425	10^7 J	Cold-side energy holdup
	3	−5.4825	10^7 J	
$E_{h,k}$	1	−1.4160	10^7 J	
	2	−1.2629	10^7 J	Hot-side energy holdup
	3	−1.0557	10^7 J	
$T_{c,k}$	1	314.132	K	
	2	315.602	K	Cold-side stage temperature
	3	317.773	K	
$T_{h,k}$	1	326.389	K	
	2	332.874	K	Hot-side stage temperature
	3	342.018	K	
N	H_2O	2.1638	kmol	
	CO_2	162.3078	kmol	
	CH_4	10.3863	kmol	
	F_1	11.74932	kmol	Flash drum component holdup
	F_2	9.5855	kmol	
	F_3	11.2516	kmol	
	F_4	8.9364	kmol	
U^e		−2.2175	10^9 J	Flash drum extensive internal energy
T_{flash}		330.25	K	Flash drum temperature
P_{flash}		10	MPa	Flash drum pressure
T_1		312.971	K	Inlet valve discharge temperature
T_2		303.65	K	Condenser outlet temperature
P_d		60	MPa	Pump discharge pressure
T_d		354.702	K	Pump discharge temperature
$T_{h,i}$		354.874	K	Top valve discharge temperature
T_{bot}		329.368	K	Bottom valve discharge temperature
W		4.246	MW	Pump power
Q_{flash}		5.676	MW	Drum heating rate
Q_{cool}		−5.462	MW	Condenser cooling rate
x_v		0.5	-	Inlet valve opening
$x_{v,t}$		0.49828	-	Top valve opening
$x_{v,b}$		0.50131	-	Bottom valve opening

Appendix B. Particle Filter Algorithm

The particle filter algorithm implemented in this work is given by Algorithm A1. In this algorithm, X_k^i and w_k^i represent the *i*-th particle and its correspondent weight at time *k*, y_k represents system measurement at time *k*, ψ_j represents probability distribution of *j*-th parameter conditioned to the state and previous parameters, f represents the state evolution law, g represents the likelihood function, N_{part} is the number of particles, and c is the filter resampling rate. The resampling algorithm used was the systematic resampling, described in Speekenbrink [27].

Algorithm A1: PNRERB-MC-DDPG method Particle filter (adapted from Speekenbrink [27])

Data: $[X_{k-1}^i, w_{k-1}^i]$, y_k, ψ_j $(j = 1, \cdots, n_\psi)$, f, g, N_{part}, c

Result: $[X_k^i, w_k^i]$

```
// A priori calculations
```

1 **for** $i \leftarrow 1$ **to** N_{part} **do**

2    $p_\psi^i \leftarrow 1$; `// initialize transition probability`

3   **for** $j \leftarrow 1$ **to** n_ψ **do**

4   Sample $\Psi_{k-1,j}^i \sim \psi_j(p_j | X_{k-1}^i, \Psi_{k-1,1}^i, \cdots, \Psi_{k-1,j-1}^i)$;

5      $p_\psi^i \leftarrow p_\psi^i \psi_j(\Psi_{k-1,j}^i | X_{k-1}^i, \Psi_{k-1,1}^i, \cdots, \Psi_{k-1,j-1}^i)$; `// calculate joint probability of`
       `sampled parameters`

6    $X_k^i \leftarrow f(X_{k-1}^i, \Psi_{k-1,1}^i, \cdots, \Psi_{k-1,n_\psi}^i)$; `// propagate particle in sampled path`

7    $w_k^i \leftarrow w_{k-1}^i p_\psi^i$; `// update weight with probability of sampled path`

8 $\xi \leftarrow \sum_{i=1}^{N_{part}} w_k^i$;

9 $w_k^i \leftarrow w_k^i / \xi$, $i = 1, \cdots, N_{part}$;

```
// A posteriori calculations
```

10 $w_k^i \leftarrow w_k^i g(y_k | X_k^i)$, $i = 1, \cdots, N_{part}$;

11 $\xi \leftarrow \sum_{i=1}^{N_{part}} w_k^i$;

12 $w_k^i \leftarrow w_k^i / \xi$, $i = 1, \cdots, N_{part}$;

13 $N_{eff} \leftarrow 1 / \sum_{i=1}^{N_{part}} (w_k^i)^2$;

14 **if** $N_{eff} < cN_{part}$ **then**

15    $[X_k^i, w_k^i] \leftarrow \text{Resample}(X_k^i, w_k^i)$;

References

1. Rausand, M.; Høyland, A. *System Reliability Theory: Models, Statistical Methods, And Applications*; John Wiley & Sons: Hoboken, NJ, USA, 2004; Volume 396.
2. Heng, A.; Zhang, S.; Tan, A.C.; Mathew, J. Rotating machinery prognostics: State of the art, challenges and opportunities. *Mech. Syst. Signal Process.* **2009**, *23*, 724–739. [CrossRef]
3. Jardine, A.K.; Lin, D.; Banjevic, D. A review on machinery diagnostics and prognostics implementing condition-based maintenance. *Mech. Syst. Signal Process.* **2006**, *20*, 1483–1510. [CrossRef]
4. Lei, Y.; Li, N.; Guo, L.; Li, N.; Yan, T.; Lin, J. Machinery health prognostics: A systematic review from data acquisition to RUL prediction. *Mech. Syst. Signal Process.* **2018**, *104*, 799–834. [CrossRef]
5. Roemer, M.J.; Byington, C.S.; Kacprzynski, G.J.; Vachtsevanos, G.; Goebel, K. Prognostics. In *System Health Management*; John Wiley & Sons, Ltd.: Hoboken, NJ, USA, **2011**, *17*, 281–295.
6. Banjevic, D. Remaining useful life in theory and practice. *Metrika* **2009**, *69*, 337–349. [CrossRef]
7. Kothamasu, R.; Huang, S.H.; VerDuin, W.H. System health monitoring and prognostics—A review of current paradigms and practices. *Int. J. Adv. Manuf. Technol.* **2006**, *28*, 1012–1024. [CrossRef]
8. Jouin, M.; Gouriveau, R.; Hissel, D.; Péra, M.C.; Zerhouni, N. Particle filter-based prognostics: Review, discussion and perspectives. *Mech. Syst. Signal Process.* **2016**, *72*, 2–31. [CrossRef]
9. de Medeiros, J.L.; de Oliveira Arinelli, L.; Teixeira, A.M.; Araújo, O.d.Q.F. *Offshore Processing of CO$_2$-Rich Natural Gas with Supersonic Separator: Multiphase Sound Speed, CO$_2$ Freeze-Out and HYSYS Implementation*; Springer: New York, NY, USA, 2018.
10. Passarelli, F.M. Processo e Sistema Para RemoçãO De DióXido de Carbono em Fase Densa de Correntes de PetróLeo e GáS Natural. BR 102014002291 A2, 2017. (In Portuguese)

11. Passarelli, F.M.; Moura, D.A.G.; Bidart, A.M.F.; Silva, J.P.; Vieira, A.J.M.; Frutuoso, L.F.A. HISEP: A Game Changer to Boost the Oil Production of High GOR and High CO Content Reservoirs. In Proceedings of the Offshore Technology Conference Brasil, Rio de Janeiro, Brazil, 30 October 2019.

12. Souza, A.F.F. Separação Submarina óleo/CO_2: Concepção Tecnológica, Modelagem, e Controle Avançado. Master's Thesis, Programa de Engenharia Química, COPPE, Universidade Federal do Rio de Janeiro, Brazil, 2018. (In Portuguese)

13. Souza, A.F.F.; Secchi, A.R.; de Souza, M.B., Jr. CO_2 Subsea Separation: Concept & Control Strategies. *IFAC-PapersOnLine* **2019**, *52*, 790–795.

14. Pereira, E.B.; Galvao, R.K.H.; Yoneyama, T. Model Predictive Control using Prognosis and Health Monitoring of actuators. In Proceedings of the 2010 IEEE International Symposium on Industrial Electronics, Bari, Italy, 4–7 July 2010; pp. 237–243. [CrossRef]

15. Escobet, T.; Puig, V.; Nejjari, F. Health Aware Control and model-based Prognosis. In Proceedings of the 2012 20th Mediterranean Conference on Control & Automation (MED), Barcelona, Spain, 3–6 July 2012; pp. 691–696. [CrossRef]

16. Sanchez, H.; Escobet, T.; Puig, V.; Odgaard, P.F. Health-aware Model Predictive Control of Wind Turbines using Fatigue Prognosis. *IFAC-PapersOnLine* **2015**, *48*, 1363–1368. [CrossRef]

17. Grosso, J.M.; Ocampo-Martinez, C.; Puig, V. Reliability–based economic model predictive control for generalised flow–based networks including actuators' health–aware capabilities. *Int. J. Appl. Math. Comput. Sci.* **2016**, *26*, 641–654. [CrossRef]

18. Verheyleweghen, A.; Jäschke, J. Framework for Combined Diagnostics, Prognostics and Optimal Operation of a Subsea Gas Compression System * *This work is funded by the SUBPRO center for research based innovation, www.ntnu.edu/subpro. *IFAC-PapersOnLine* **2017**, *50*, 15916–15921. [CrossRef]

19. Verheyleweghen, A.; Gjøby, J.M.; Jäschke, J. Health-Aware Operation of a Subsea Compression System Subject to Degradation. In Proceedings of the 28th European Symposium on Computer Aided Process Engineering, Graz, Austria, 10–13 June 2018; pp. 1021–1026. [CrossRef]

20. Bernardino, L.F. Health-Aware Control and Model-Based Prognostics of a Subsea Oil and Gas Separation System. Master's Thesis, Programa de Engenharia Química, COPPE, Universidade Federal do Rio de Janeiro, Brazil, 2019.

21. Abrahams, D.; Grosse-Kunstleve, R.W.; Overloading, O. Building hybrid systems with Boost.Python. *C/C++ Users J.* **2003**, *21*, 29–36.

22. Python, version 3.7, Python Software Foundation, Beaverton, Oregon, USA, 2018.

23. Andersson, C.; Führer, C.; Åkesson, J. Assimulo: A unified framework for ODE solvers. *Math. Comput. Simul.* **2015**, *116*, 26–43. [CrossRef]

24. Simon, D. *Optimal State Estimation: Kalman, H Infinity, and Nonlinear Approaches*; John Wiley & Sons: Hoboken, NJ, USA, 2006.

25. Virtanen, P.; Gommers, R.; Oliphant, T.E.; Haberland, M.; Reddy, T.; Cournapeau, D.; Burovski, E.; Peterson, P.; Weckesser, W.; Bright, J.; et al. SciPy 1.0–Fundamental Algorithms for Scientific Computing in Python. *arXiv* **2019**, arXiv:1907.10121.

26. Seborg, D.E.; Mellichamp, D.A.; Edgar, T.F.; Doyle, F.J., III. *Process Dynamics and Control*; John Wiley & Sons: Hoboken, NJ, USA, 2011.

27. Speekenbrink, M. A tutorial on particle filters. *J. Math. Psychol.* **2016**, *73*, 140–152. [CrossRef]

28. Paris, P.; Erdogan, F. A critical analysis of crack propagation laws. *J. Basic Eng.* **1963**, *85*, 528–533. [CrossRef]

29. Rawlings, J.B.; Angeli, D.; Bates, C.N. Fundamentals of economic model predictive control. In Proceedings of the 2012 IEEE 51st IEEE Conference on Decision and Control (CDC), Maui, HI, USA, 10–13 December 2012; pp. 3851–3861.

30. Gembicki, F.; Haimes, Y. Approach to performance and sensitivity multiobjective optimization: The goal attainment method. *IEEE Trans. Autom. Control* **1975**, *20*, 769–771. [CrossRef]

31. Skogestad, S. Simple analytic rules for model reduction and PID controller tuning. *J. Process Control* **2003**, *13*, 291–309. [CrossRef]